

# Order–Disorder and Order–Order Transitions in Mixtures of Highly Asymmetric Triblock Copolymer and Low Molecular Weight Homopolymers

Seung-Heon Lee and Kookheon Char\*

School of Chemical Engineering, Seoul National University, Seoul 151-742, Korea

Ginam Kim†

Department of Chemical, Biochemical, and Materials Engineering, Stevens Institute of Technology, Hoboken, New Jersey 07030

Received April 14, 2000

**ABSTRACT:** The order–disorder and order–order transitions (ODT and OOT) of a series of mixtures of a compositionally asymmetric polystyrene-*block*-polyisoprene-*block*-polystyrene copolymer (SIS) ( $f_{PS} = 0.131$ ) and low molecular weight PS homopolymers with different molecular weights have been investigated by using transmission electron microscopy (TEM), synchrotron small-angle X-ray scattering (SAXS), and rheology. ODT temperatures determined from the discontinuous change in  $1/I_{max}$  and  $\sigma_q^2$  vs  $1/T$  plots were found to be in reasonable proximity to the ones determined from the discontinuous change in  $\log G'$  vs  $T$  plots. Various OOT's were also identified for a few of V4113/PS mixtures, as evidenced from both SAXS and rheology. This was further confirmed by TEM for the quenched samples. Spherical microdomains in liquidlike packing (LLP) observed for pure V4113 at low temperature were found not to be an equilibrium phase, which would transform completely to spheres in body-centered-cubic array (BCC) with prolonged annealing time. Our asymmetric SIS/low molecular weight PS mixtures showed a minimum ODT around 10 wt % of PS. This unusual phase behavior has not been observed experimentally in any block copolymer/homopolymer mixture system and is also inconsistent with any existing theoretical predictions. We believe that this is related to the fact that the styrene volume fraction of our SIS triblock copolymer is quite close to the transition boundary between cylinders in hexagonal array (HEX) and BCC. In this case, the chain stretching and/or packing frustration effects, which are usually ignored in normal block copolymer/homopolymer mixtures, can be significant with the addition of low molecular weight homopolymer to the minor phase of the highly asymmetric triblock copolymer.

## 1. Introduction

Block copolymer/homopolymer mixtures have been of considerable interest because they can be easily modified to yield desired properties in polymeric materials such as pressure-sensitive adhesives. Phase behavior of these mixtures is generally quite complicated because two different natures of transition can occur at the same time: *macrophase* and *microphase* separation. If the molecular weight of homopolymer is sufficiently low compared with that of block copolymer, it tends to be solubilized into one of the microdomains.<sup>1–4</sup> In this case, the macrophase separation is suppressed, and the microphase separation (or *order–disorder transition*; ODT) becomes dominant.

There have been many theoretical and experimental works on the ODT of pure block copolymers.<sup>5–12</sup> A few researchers have also investigated the ODT of block copolymer/homopolymer mixtures. Whitmore and Noolandi<sup>1</sup> calculated the theoretical phase diagrams of AB diblock copolymer/A homopolymer mixtures using functional integral formalism. They assumed that the ordered phase has a lamellar structure, so that the third-order term in the Landau–Ginzburg expansion of free energy vanishes. They found that the spinodal ODT temperature decreases with the addition of homopoly-

mer if the degree of polymerization of A homopolymer is smaller than the half of that of A block of symmetric AB diblock copolymer. de la Cruz and Sanchez<sup>13</sup> also investigated theoretically the effect of the relative molecular weight and the composition of homopolymer on spinodal ODT by modifying the scattering theory, originally proposed by Leibler,<sup>5</sup> for AB diblock copolymer/A homopolymer mixtures, and obtained similar results with those of Whitmore and Noolandi. Recently, several researchers extended the self-consistent mean-field calculations to block copolymer/homopolymer mixtures having ordered phases other than lamellae. Matsen<sup>14</sup> found that the addition of homopolymer stabilizes the complex ordered phases in the weak segregation regime. Janert and Schick<sup>15</sup> investigated the effect of relative homopolymer length on the phase behavior in the weak to the intermediate segregation regime considering lamellae, hexagonal, and body-centered-cubic phases. ODT behavior in previous authors' works, however, showed the similar trend to that obtained from the calculations just assuming the lamellar phase.

Experimentally, Bodycomb et al.<sup>16</sup> examined the ODT of binary mixtures of symmetric styrene–isoprene (SI) diblock copolymers ( $f_{PS} \sim 0.5$ ) with different molecular weights and a PS homopolymer using small-angle X-ray scattering (SAXS) measurements. Their ODT showed either an increasing or a decreasing trend with the addition of PS depending on the molecular weight of the block copolymer used, which is in agreement with theoretical predictions. The ODT and phase behavior

\* To whom correspondence should be addressed. E-mail: khchar@plaza.snu.ac.kr.

† Current address: Dow Corning Corporation, Midland, MI 48686.

**Table 1. Molecular Characteristics of the Polymers Used in This Study**

sample	$M_w^a \times 10^{-3}$ (g/mol) (PS- <i>b</i> -PI- <i>b</i> -PS)	$M_w/M_n^a$	PS (wt %) <sup>b</sup>	$T_{g,PS}^c$ (°C)
V4113	15.3- <i>b</i> -171.7- <i>b</i> -15.3	1.19 <sup>d</sup>	15.1	
PS2	1.9	1.09	100	69
PS3	2.9	1.06	100	74
PS6	5.9	1.04	100	86
PS11	11.4	1.03	100	90

<sup>a</sup> Determined from GPC in THF with PS standards. <sup>b</sup> Determined from H NMR. <sup>c</sup> Determined from the second scan of DSC at a heating rate of 10 °C/min. <sup>d</sup> 18 wt % of uncoupled diblocks is present in V4113.

of the mixtures with compositionally asymmetric block copolymers have also been studied by a few researchers. Roe and Zin<sup>17</sup> investigated the phase behavior of mixtures of styrene–butadiene (SB) diblock copolymer ( $w_{PS} = 0.27$ , where  $w_{PS}$  is the weight fraction of PS) and polystyrene or polybutadiene homopolymers with different molecular weights using SAXS and turbidity measurements. Baek et al.<sup>18</sup> investigated the ODT and phase behavior of mixtures of SIS triblock copolymers ( $w_{PS} = 0.13$  and  $0.30$ ) and PS homopolymers by using turbidity and rheological measurements. To the best of our knowledge, however, systematic studies on the order–disorder and order–order transitions in mixtures of *compositionally asymmetric* block copolymer and *low molecular weight* homopolymers have yet to be done. Since relatively high molecular weight homopolymers were used in the previous works, the ODT temperature just increased as the homopolymer weight fraction was increased, and eventually macrophase separation occurred above a critical value of composition that was quite small.

In present study, we employed transmission electron microscopy (TEM), SAXS, and rheological measurements to investigate the order–disorder and order–order transitions in a series of mixtures of a *compositionally asymmetric* SIS triblock copolymer and low molecular weight PS homopolymers, which did not show macrophase separation in the whole temperature and composition range covered in this experiment. Phase diagrams obtained from both measurements were compared with the predictions based on the self-consistent mean-field theory.<sup>1</sup> The difference between theoretical prediction and experimental results is discussed.

## 2. Experimental Section

**Materials.** A commercial grade of polystyrene-*block*-polyisoprene-*block*-polystyrene (SIS) copolymer, Vector 4113 (DEX-CO Polymers), was used as received. This triblock copolymer is highly asymmetric in block composition, containing 15.1 wt % of PS. It will be denoted, hereafter, as V4113. Four polystyrenes (PS) with different molecular weights were synthesized by anionic polymerization using *n*-butyllithium as an initiator and benzene containing a trace amount of tetrahydrofuran as a solvent. The characteristics of these polymers are summarized in Table 1. The weight-average molecular weight,  $M_w$ , and the polydispersity index,  $M_w/M_n$ , were determined by gel permeation chromatography (GPC) using PS standards, and the PS weight percent of the block copolymer was determined by proton nuclear magnetic resonance (H NMR). The microstructure of PI block of the block copolymer was determined to be 93% of 1,4 addition and 7% of 3,4 addition by H NMR. The glass transition temperature of polystyrenes,  $T_{g,PS}$ , was measured from the second scan of differential scanning calorimetry (DSC) at a heating rate of 10 °C/min.

**Sample Preparation.** Mixture samples were prepared by solution casting with toluene as a solvent. Predetermined amounts of block copolymers and PS homopolymers were first dissolved in toluene (below 8 wt %) with 0.3 wt % antioxidant (Irganox 1010, Ciba-Geigy Group). The solvent was slowly evaporated at ambient condition for 3 weeks and then in a vacuum oven at 55 °C for 3 days. Finally, all the samples were annealed in a vacuum oven for 3 days at 130 °C, which is well above  $T_{g,PS}$ . GPC curves of the samples before and after annealing were found to be nearly identical, implying that there was no appreciable degradation after annealing.

**Rheology.** Two different experimental measurements, rheology and SAXS, were used to determine the order–disorder transition temperature ( $T_{ODT}$ ) of each mixture. RMS 800 (Rheometrics Inc.) in parallel plate geometry with 25 mm diameter and 1.5 mm gap was used to measure the dynamic viscoelastic storage and loss moduli,  $G'$  and  $G''$ , of the mixtures as a function of temperature. A heating rate of 1 °C/min was used, and the strain amplitude was small enough to ensure linear viscoelasticity (typically smaller than 5%) for all the measurements. All measurements were carried out under nitrogen blanket in order to prevent oxidative degradation of the samples. GPC measurements after temperature sweep indicated that degradation problem in our samples is not serious.

**Small-Angle X-ray Scattering (SAXS).** Synchrotron SAXS measurements were carried out at 4C2 SAXS beamline in Pohang Light Source (PLS), Korea, which consisted of 2 GeV LINAC accelerator, storage ring, Si(111) double crystal monochromator, ion chambers, and one-dimensional position-sensitive detector with 2048 pixels. The wavelength ( $\lambda$ ) of the synchrotron beam was 1.59 Å, and the energy resolution ( $\Delta\lambda/\lambda$ ) was  $5 \times 10^{-4}$ . Typical beam size was smaller than  $1 \times 1$  mm<sup>2</sup>. Sample-to-detector distance was 103.7 cm. Scattering profiles were obtained as a function of temperature at a heating rate of 1 °C/min and then corrected for absorption, air scattering, and inelastic film scattering. Before the heating run, each sample was maintained for about 20 min at a specified temperature, which is above  $T_{g,PS}$ , to obtain thermal equilibrium. Nitrogen was purged during the measurements in order to prevent oxidative degradation of the samples. To obtain information on the change in the microdomain morphology with the addition of PS homopolymer, room-temperature SAXS measurements were also carried out for pure block copolymer and block copolymer/homopolymer mixture samples quenched after annealing at 130 °C for 3 days.

**Transmission Electron Microscopy (TEM).** TEM was employed to identify the microdomain morphology of the samples quenched from a specified temperature. Electron transparent films of the quenched samples with nominal thicknesses of 50–80 nm were cryo-microtomed at –90 °C using a diamond knife on a Leica Ultracut UCT and transferred to carbon film coated Cu grids. The specimens were stained by exposure for 20 min to osmium tetroxide (OsO<sub>4</sub>) vapor from OsO<sub>4</sub> crystal warmed to 50 °C. Since OsO<sub>4</sub> reacts preferentially with unsaturated carbon double bonds in the polyisoprene block, the stained polyisoprene phase appears dark in a bright-field TEM micrograph. In all micrographs presented here, the PI phase appears dark and the PS phase appears bright. TEM was performed on a Philips CM30 Super Twin TEM at Stevens Institute of Technology.

## 3. Results and Discussion

**Solubility of PS in the Microdomains of SIS Triblock Copolymer.** Before jumping directly into the discussion of the order–disorder and order–order transition of block copolymer/homopolymer mixtures, we should first check the molecular miscibility between an SIS triblock copolymer and a series of PS homopolymers. We conducted the hot stage microscopy for this purpose. It was found that V4113/PS mixtures with low molecular weight PS's (PS2 and PS3) did not show any macrophase separation up to 40 wt % of PS. On the

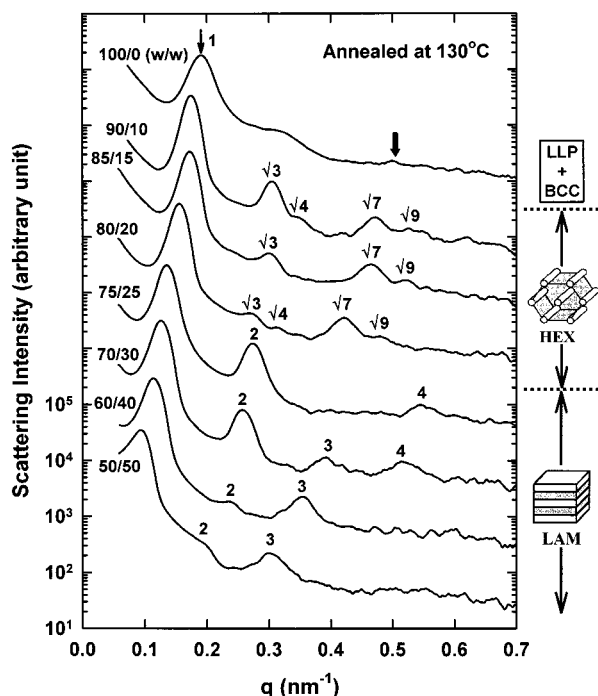


**Figure 1.** Synchrotron SAXS profiles of V4113/PS2 mixtures with different composition at room temperature after annealing the samples at 130 °C for 3 days. Each data set was vertically shifted for clarity.

other hand, the mixtures with high molecular weight PS's (PS6 and PS11) were found to exhibit macrophase separation when PS weight fraction exceeded 0.3 and 0.2, respectively. It has been reported by many investigators that the homopolymer solubility in block copolymer microdomain decreases with increasing the molecular weight of a homopolymer added.<sup>1,4,17,18</sup> It should be emphasized here that in present work we only focus on the order-disorder and order-order transition behavior of the mixtures in the composition range showing no macrophase separation.

**Change in Equilibrium Microdomain Morphology of SIS Triblock Copolymer with the Addition of PS Homopolymer.** It is well-known that a block copolymer shows multiple *interparticle* scattering peaks (Bragg reflection peaks) due to its periodic microdomain structure having a long-range order as well as the *intraparticle* scattering peaks (form factor) due to its isolated single microdomain.<sup>2,12</sup> Information on the microdomain morphology of a block copolymer can be obtained from the relative positions of these multiple Bragg peaks, since they exhibit different arrays depending on the shape of the microdomain structure, e.g., 1, 2, 3, 4, ... for lamellae (LAM), 1,  $\sqrt{3}$ ,  $\sqrt{4}$ ,  $\sqrt{7}$ ,  $\sqrt{9}$ , ... for cylinders in hexagonal array (HEX), 1,  $\sqrt{2}$ ,  $\sqrt{3}$ ,  $\sqrt{4}$ ,  $\sqrt{5}$ , ... for spheres in body-centered-cubic array (BCC), and so forth.

Synchrotron SAXS measurements were carried out at room temperature in order to obtain the information on the change of the equilibrium microdomain morphology of SIS/PS mixtures with PS addition. In Figure 1, the results for V4113/PS2 mixtures are presented in a semilogarithmic plot of scattered intensity as a function of scattering wavenumber  $q$ . Here,  $q$  is given by

$$q = (4\pi/\lambda) \sin(\theta/2) \quad (1)$$

where  $\lambda$  is the wavelength of the X-ray and  $\theta$  is the

scattering angle. All the measurements were taken for the samples quenched to room temperature after annealing at 130 °C for 3 days in a vacuum oven. Each data set was vertically shifted for clarity. As shown in Figure 1, the relative positions of scattering peaks of V4113/PS2 mixtures are 1,  $\sqrt{3}$ ,  $\sqrt{4}$ , and  $\sqrt{7}$  up to 20 wt % of PS2, while 1, 2, 3, and 4 above it. As a consequence, we can tentatively assign HEX morphology to the former case and LAM morphology to the latter case based on the SAXS results. It is also interesting to observe in Figure 1 that a certain higher order peak is selectively suppressed due to the overlap of the maximum in Bragg peak and the minimum in form factor;<sup>19,20</sup> the peak at a relative position  $\sqrt{4}$  is suppressed for the 85/15 mixture, and the peak at a relative position 3 is suppressed for the 75/25 mixture. This scattering peak extinction is governed by the volume fraction of the block copolymer, thus by the overall styrene volume fraction for our block copolymer/homopolymer mixture system. For example, it has been reported that the second-order peak is suppressed for a symmetric AB diblock copolymer ( $f_A \sim 0.5$ , where  $f_A$  is the volume fraction of A block) having LAM morphology.<sup>19</sup>

To confirm the exact microdomain morphologies of V4113/PS2 mixtures, we independently carried out TEM for the same samples used for SAXS measurements. Figure 2 shows a series of TEM micrographs for 100/0, 90/10, 80/20, and 70/30 (w/w) V4113/PS2 mixture samples prepared by quenching them to room temperature after annealing at 130 °C for 3 days in a vacuum oven. In the TEM micrographs, the polyisoprene (PI) phase appears dark and the polystyrene (PS) phase appears bright since the staining agent OsO<sub>4</sub> used in present work preferentially reacts with double bonds of PI block. It can be clearly seen from the figure that 90/10 and 80/20 (w/w) mixtures have HEX phases (Figure 2, b and c, respectively) while 70/30 (w/w) mixture has an alternating LAM phase (Figure 2d). The TEM micrograph of a 75/25 (w/w) mixture also showed LAM phase (not shown here). These TEM results support the morphology assignment solely based on the SAXS data, and it can be inferred from both results that the transition from HEX to LAM phase occurs in the range of  $0.20 < w_{PS2} < 0.25$ , where  $w_{PS2}$  is the weight fraction of PS2 in the mixture. If we assume complete solubilization of PS2 in the polystyrene microdomains of an SIS triblock copolymer, the overall styrene volume fraction  $\Phi_{PS}$  at the annealing temperature can be calculated. The value of  $\Phi_{PS}$  at the transition boundary,  $0.288 < \Phi_{PS} < 0.328$ , is in reasonable agreement with that of PS volume fraction of SI diblock copolymers ( $0.32 < f_{PS} < 0.35$ ) reported in the literature<sup>9</sup> except the fact that it is slightly shifted to a lower value compared with the value of SI diblock copolymers. As a result, it can be concluded that  $\Phi_{PS}$  is a good measure of equilibrium microdomain morphology in block copolymer/homopolymer mixtures.

It should be noted here that TEM micrograph of pure V4113 (Figure 2a) shows a complex microdomain morphology unlike other mixture samples. It shows the coexistence of two different morphologies and many grain boundaries between them: (111) projection of BCC in the upper-left part of Figure 2a, (110) projection of BCC in the upper-right part, (100) projection of BCC in the middle part, and spheres with *liquidlike packing* (LLP) in the lower part. The TEM micrograph with lower magnification (not shown here) reveals that the LLP phase is major. The broad first-order Bragg peak



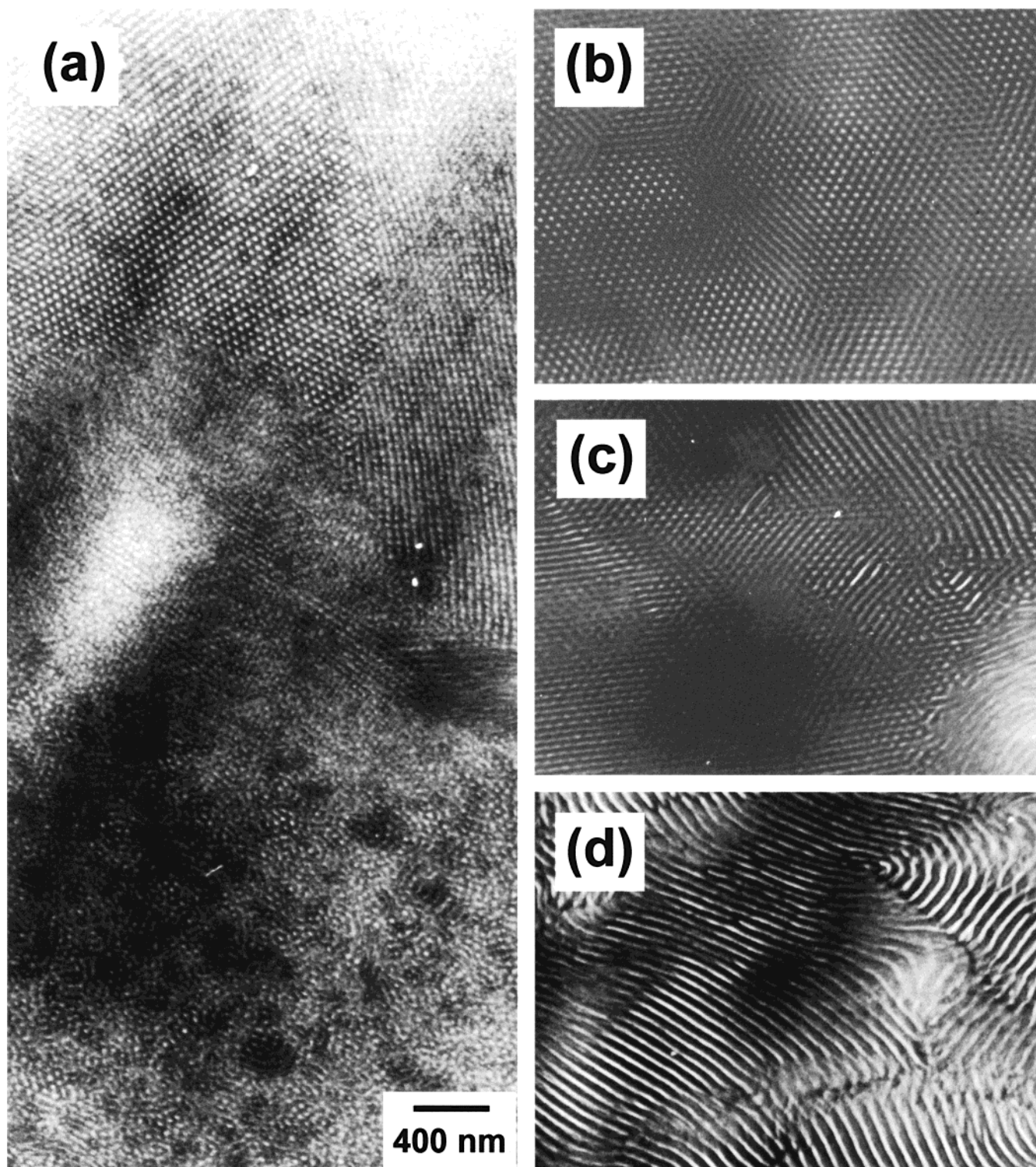


**Figure 2.** TEM micrographs of (a) 100/0, (b) 90/10, (c) 80/20, and (d) 70/30 (w/w) V4113/PS2 mixtures at room temperature after annealing the samples at 130 °C for 3 days.

indicated by a thin arrow and the suppression or absence of higher order peaks in the SAXS profile of V4113 shown at the top of Figure 1 are due to the coexistence of different phases and the lack of long-range order (i.e., the existence of LLP phase as shown in the lower part of Figure 2a). In addition to this, a very broad maximum of V4113 at  $q \sim 0.51 \text{ nm}^{-1}$  indicated by a thick arrow in Figure 1 can be attributed to the first-order *intraparticle* scattering arising from isolated single spherical microdomains in LLP phase,

satisfying  $q_m R = 5.765$  where  $R$  is the average radius of spheres.<sup>2</sup> A broad shoulder at  $q \sim 0.33 \text{ nm}^{-1}$  is due to the combination of the intraparticle scattering, i.e., the tail of the zeroth-order form factor, and the interparticle scattering from LLP and BCC spheres as predicted by the paracrystal model with a very large distortion.<sup>21,22</sup> The value of  $R$  was calculated to be about 11 nm using the above equation. This is in complete match with the radius of BCC spheres ( $R \sim 11 \text{ nm}$ ) calculated from the domain periodicity  $D (= 2\pi/q_{\text{max}}$ ,

where  $q_{\max}$  is the wavenumber at which scattering intensity is maximum) by assuming complete BCC packing. In addition, this is, within experimental uncertainties, in reasonable agreement with the value ( $R \sim 12$  nm) obtained from the TEM micrograph of the LLP phase shown in Figure 2a.

There is one thing worth mentioning at this point. When preparing block copolymer samples by solution casting as in our case, care should be taken on the choice of solvent since a slight selectivity of the solvent can significantly affect the microdomain morphology. Funaki et al.<sup>23</sup> investigated the influence of casting solvents on the microphase-separated structures of two *asymmetric* poly(2-vinylpyridine)-polyisoprene (P2VP-PI) copolymers ( $f_{\text{P2VP}} = 0.12$  and  $0.16$ ) and found that microdomain morphologies obtained even after a long-time annealing above  $T_g$  are quite different depending on the solvent used. They attributed this to the vitrification of the nonequilibrium microdomain structures developed during the solvent casting process. Lipic et al.<sup>24</sup> also reported similar results for a poly(ethylene)-poly(ethylene) (PE-PEE) diblock copolymer and binary diblock blends with overall PE compositions of 0.44, 0.46, and 0.48. They found a difference between the morphologies prepared by solution casting with decahydronaphthalene and by melt pressing even after extended annealing time (6 days at 150 °C) when the overall volume fraction is near the LAM/HEX transition boundary. Although toluene used in our study has been widely accepted as a nonselective solvent for block copolymers made of PS and PI, it has recently been reported to be slightly selective toward PI.<sup>25</sup> This slight selectivity would cause more swelling of PI phase than PS phase in our system during the casting process, thus decreasing effective  $f_{\text{PS}}$ . If the solvent evaporation rate is fast enough, nonequilibrium LLP morphology can be induced for highly asymmetric block copolymers such as our V4113. Although the solvent evaporation was carried out over 3 weeks at room temperature during our sample preparation, it can be faster than the LLP  $\rightarrow$  BCC ordering rate. Therefore, we concluded that the LLP phase in pure V4113 throughout the whole area of TEM observation is a nonequilibrium morphology induced by the solvent casting process, and the BCC phase found in some parts of TEM images is the equilibrium morphology induced by the annealing process. It seems that the annealing time (3 days) is not sufficient for the highly asymmetric V4113 sample to fully achieve equilibrium BCC morphology at the annealing temperature of 130 °C although the temperature is well above  $T_{g,\text{PS}}$ . Recent work by Yamaguchi et al.<sup>26</sup> is quite informative to our results since the morphology of their asymmetric PS-PI diblock copolymer having  $f_{\text{PS}} = 0.18$ , which is quite similar to ours, transformed completely from LLP to BCC after quite a long time annealing (15 days) at about 30 °C above  $T_{g,\text{PS}}$ .

**ODT and OOT Determined from Rheology.** To determine the order-disorder transition temperature ( $T_{\text{ODT}}$ ), two different measurements, i.e., rheology and SAXS, were employed in present study. Rheological measurements were first carried out. Figure 3 shows  $\log G'$  vs  $T$  plots of V4113/PS2 mixtures with different composition. Angular frequency  $\omega$  was fixed to 0.1 rad/s for all the samples except for 80/20 and 60/40 (w/w) mixtures with 0.2 rad/s, and the heating rate was 1 °C/min. Each data set was vertically shifted by multiplying  $10^5$ ,  $10^4$ ,  $10^3$ ,  $10^2$ ,  $10^1$ , and  $10^0$  for clarity. As evident

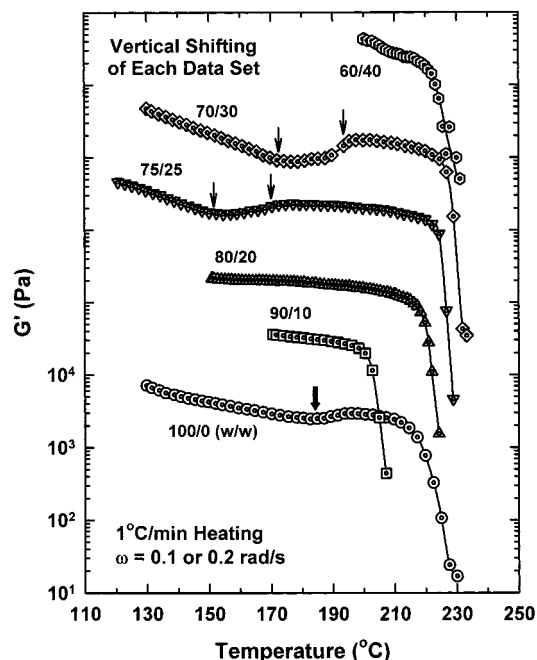


**Figure 3.** Dynamic storage modulus ( $G'$ ) as a function of temperature for V4113/PS2 mixtures with different composition. Each data set was vertically shifted by multiplying  $10^5$ ,  $10^4$ ,  $10^3$ ,  $10^2$ ,  $10^1$ , and  $10^0$  for clarity.

from the figure,  $G'$  shows a precipitous drop at a certain temperature for each mixture sample. Rosedale and Bates<sup>7</sup> investigated the order-disorder transition behavior of a series of PEP-PEE block copolymers having lamellar microdomains and found that both  $G'$  and  $G''$  drop precipitously at a certain temperature with angular frequencies below critical angular frequencies ( $\omega_c'$  and  $\omega_c''$ , respectively). They also reported that the drop in  $G'$  is more pronounced since the critical angular frequency for  $G'$  is larger than that for  $G''$  (i.e.,  $\omega_c' > \omega_c''$ ). Following their criterion, the temperature at which there is an abrupt change in  $G'$  was chosen as  $T_{\text{ODT}}$  of each mixture. It is interesting to note that  $T_{\text{ODT}}$  of V4113/PS2 mixtures first decreases up to 10 wt % and increases again. This unusual phase behavior will be discussed later.

In Figure 3, the  $\log G'$  vs  $T$  plot for pure V4113 shows a local minimum around 185 °C indicated by a thick arrow below the ODT temperature. Many researchers<sup>9,27</sup> have related this type of local minimum or other changes in  $\log G'$  vs  $T$  plots to the OOT of block copolymer system based on their TEM, SAXS, and rheological measurements. We note that Ryu et al.<sup>27</sup> recently reported the abrupt change in  $\log G'$  vs  $T$  plot for the HEX/BCC transition of an asymmetric SIS triblock copolymer having  $w_{\text{PS}} = 0.167$ , which is slightly larger than that of our triblock copolymer. However, the local minimum in  $G'$  of our V4113 sample is not believed to be due to the equilibrium OOT since the LLP phase observed at lower temperature is not an equilibrium morphology as mentioned before. We think that it rather indicates the relaxation from the nonequilibrium LLP phase to an equilibrium BCC phase, as will be further supported by SAXS and TEM in the next section. We already noted from the work by Yamaguchi et al.<sup>26</sup> in the previous section that a long-time annealing of an asymmetric PS-PI diblock copolymer eventually transformed LLP to BCC. They further found that a local minimum in  $G'$  observed during heating an unannealed



sample completely disappeared after a long-time annealing. We should, however, mention here that the existence of nonequilibrium LLP phase at lower temperature did not affect the position of precipitous drop in  $G'$  as confirmed by the above authors.

In Figure 3, the  $\log G'$  vs  $T$  plots for 75/25 and 70/30 (w/w) mixtures also show distinct changes in addition to the ODT. Unlike pure V4113, these changes are related to equilibrium OOT's. There exist two OOT's for both mixtures as indicated by thin arrows. A complete description of the microphase structure in each region will be discussed in the next section by combining SAXS and TEM results.

Recently, a few researchers argue the Bates' criterion for the determination of ODT of highly asymmetric block copolymers and proposed another method. Han and co-workers<sup>11,28</sup> argued that the discontinuous drop in  $\log G'$  vs  $T$  plots for asymmetric block copolymers signifies not ODT but the *lattice disordering transition* (LDT), above which the regular packing of cylinders or spheres is destroyed; the long-range order disappears. Instead, they have used  $\log G'$  vs  $\log G''$  plots to determine the *true* ODT temperatures of asymmetric SI diblock and SIS triblock copolymers and proposed that the temperature at which the  $\log G'$  vs  $\log G''$  plot no longer changes should be regarded as  $T_{\text{ODT}}$ . Their criterion was, however, not checked in detail for our V4113/PS mixture system since the values of  $T_{\text{ODT}}$  determined from the  $\log G'$  vs  $\log G''$  plots are usually much higher than those determined from the  $\log G'$  vs  $T$  plots and exceed the thermal degradation limit of our system ( $\sim 250^\circ\text{C}$ ). In addition to this, ODT's and LDT's of SIS/PS mixtures recently studied by them were found to show the same trend with the addition of PS over the whole composition range although the ODT was higher than the LDT by about 20–30  $^\circ\text{C}$ .<sup>29</sup> This means that the differentiation between ODT and LDT for our SIS/PS mixtures does not really matter since we are only concerned with the change of a transition, whether it is ODT or LDT, due to the addition of PS. A detailed discussion on the ODT and LDT is beyond the scope of current paper and deserves a separate research with more well-defined block copolymers.

#### ODT and OOT Determined from SAXS and TEM.

Figure 4 shows the typical change in synchrotron SAXS profiles of pure V4113 with temperature. Scattering intensity is plotted in logarithmic scale in order to clearly see the change in multiple scattering peaks. Maximum scattered intensity  $I_{\text{max}}$  shows a sharp decrease between 225 and 230  $^\circ\text{C}$ . This discontinuity is more pronounced when the inverse of the scattering maximum  $1/I_{\text{max}}$  and the square of the half-width at half-maximum  $\sigma_q^2$  were plotted against inverse temperature  $1/T$  as shown in Figure 5a. Sakamoto and Hashimoto<sup>10</sup> investigated the ODT of nearly symmetric SI diblock copolymer ( $f_{\text{PS}} = 0.45$ ) using SAXS and reported that there exists a clear discontinuity at ODT in  $1/I_{\text{max}}$  vs  $1/T$  plot. They also reported that  $\sigma_q^2$  shows the same trend as  $1/I_{\text{max}}$ . As can be seen in Figure 5a,  $\sigma_q^2$  follows exactly the same trend as  $1/I_{\text{max}}$ . We note here that the discontinuities in both  $1/I_{\text{max}}$  and  $\sigma_q^2$  vs  $1/T$  plots were reported by Bodycomb et al.<sup>16</sup> even for the ODT of block copolymer/homopolymer mixtures. From Figure 5a, the temperature at which the discontinuity occurs in both  $1/I_{\text{max}}$  and  $\sigma_q^2$  vs  $1/T$  plots was chosen as the  $T_{\text{ODT}}$  of the pure V4113. The value of the  $T_{\text{ODT}}$  is in good agreement with the one determined from

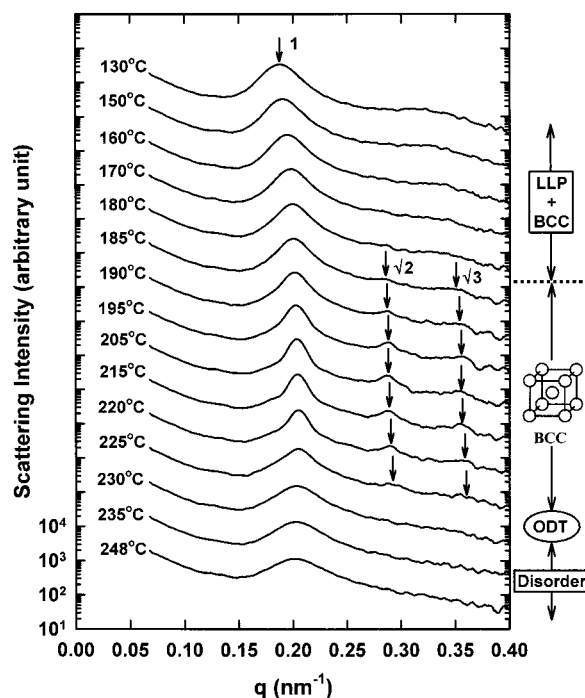


**Figure 4.** Synchrotron SAXS profiles of V4113 as a function of temperature. A heating rate of 1  $^\circ\text{C}/\text{min}$  was used. Each data set was vertically shifted for clarity.

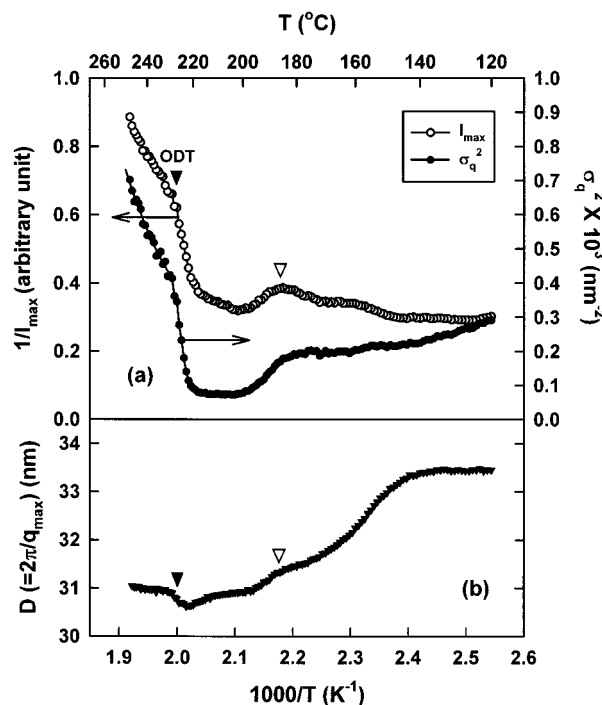


**Figure 5.** Scattering parameters as a function of inverse temperature for V4113: (a) inverse of the scattering maximum ( $1/I_{\text{max}}$ ) and square of half-width at half-maximum ( $\sigma_q^2$ ) plotted against  $1/T$ ; (b) domain spacing ( $D = 2\pi/q_{\text{max}}$ ) against  $1/T$ . A heating rate of 1  $^\circ\text{C}/\text{min}$  was used.

the precipitous decrease in the  $\log G'$  vs  $T$  plot shown in Figure 3.

In Figure 5b, the domain periodicity  $D (= 2\pi/q_{\text{max}})$  was plotted against  $1/T$ . It is interesting to note that there also exists a discontinuity in  $D$  at ODT. This is in contrary to the results of Sakamoto and Hashimoto<sup>10</sup> in which  $D$  is continuous at ODT. However, Koga et al.<sup>30</sup> recently investigated the same SI diblock copolymer as

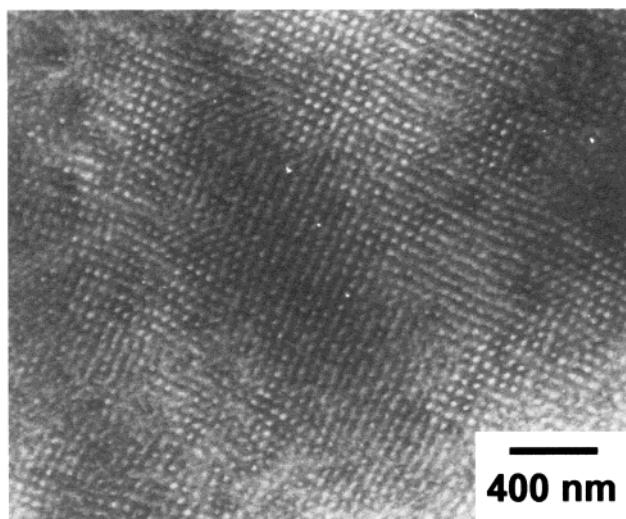


**Figure 6.** TEM micrograph of a V4113 sample quenched into liquid nitrogen after annealing at 205 °C for 30 min.

that used in ref 10 using USAXS which is more sensitive than conventional SAXS and found that there exists a small discontinuity in  $D$  at ODT. Floudas and co-workers<sup>31,32</sup> examined the ODT of an SI<sub>2</sub> simple graft copolymer, an SIB terpolymer, (SI)<sub>4</sub> star-block copolymers, and an asymmetric SI diblock copolymer using SAXS and also reported the discontinuity in  $D$  at ODT. Ogawa et al.<sup>12</sup> also reported results similar to our study for an asymmetric SI diblock copolymer with  $f_{PS} = 0.303$ .

It is clearly seen in Figure 4 that the peaks at relative positions  $\sqrt{2}$  and  $\sqrt{3}$  start to grow above 180 °C, signaling the transformation from LLP to BCC phase around this temperature. The temperature is again in good agreement with that obtained from rheological measurement in the previous section. A local maximum in  $1/I_{\max}$  vs  $1/T$  plot and a discontinuous change in  $\sigma_q^2$  vs  $1/T$  plot were also found around this temperature as shown in Figure 5a. In addition to this, a discontinuous change in  $D$  occurs at the same temperature as can be seen in Figure 5b, although the change is quite small. Many researchers<sup>28,33</sup> have related all these changes in SAXS parameters to the OOT. Sakamoto et al.<sup>28</sup> observed the local maxima in both  $1/I_{\max}$  and  $\sigma_q^2$  vs  $1/T$  plots at OOT from HEX to BCC for an asymmetric SIS triblock copolymer ( $w_{PS} = 0.183$ ). Matsen and Bates<sup>33</sup> also found that there exists the discontinuity in  $D$  at OOT by using the self-consistent-field theory (SCFT) and incorporating the conformational asymmetry of the system. Although the nonequilibrium relaxation process of V4113 from LLP to BCC also shows similar changes in SAXS parameters, there is a great difference between the forms of  $\sigma_q^2$  vs  $1/T$  plots of our V4113 and the block copolymer sample of Sakamoto et al.<sup>28</sup> In our case,  $\sigma_q^2$  does not show a local maximum but slightly decreases up to 180 °C as temperature is increased or as  $1/T$  is decreased and then shows an abrupt drop in the temperature range between 180 and 200 °C. This behavior can easily be expected since the first-order Bragg peak will become sharper, and therefore  $\sigma_q$  will be smaller when LLP transforms to BCC.

The relaxation of V4113 from LLP to BCC was further confirmed by TEM micrograph of the quenched V4113 sample as shown in Figure 6. The sample was rapidly quenched into liquid nitrogen after annealing for 30 min at 205 °C above the relaxation temperature. Annealing was carried out by using the same heating stage with

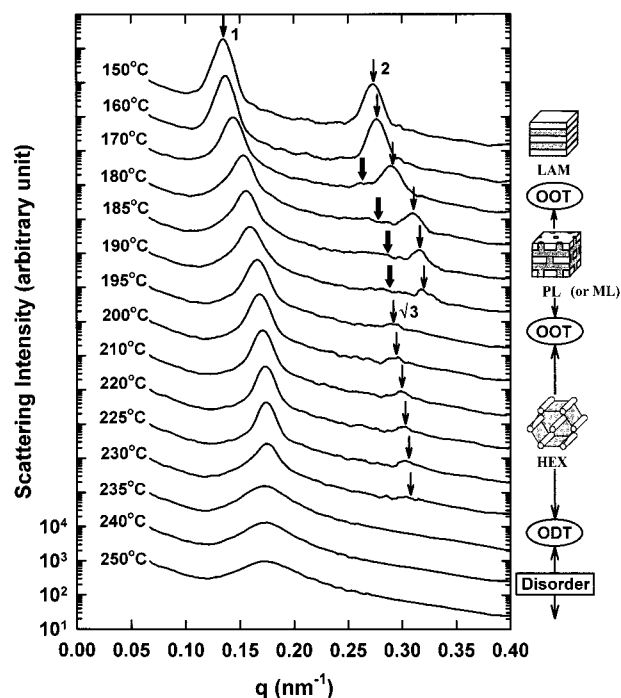


**Figure 7.** Synchrotron SAXS profiles of 70/30 (w/w) V4113/PS2 mixture as a function of temperature. A heating rate of 1 °C/min was used. Each data set was vertically shifted for clarity.

nitrogen purge as was used for SAXS measurements. Figure 6 shows clear (100) projection of BCC phase as expected from SAXS data. We have already shown in Figure 2a that LLP phase is dominant for the sample annealed at 130 °C for 3 days. From the results obtained so far, we conclude that the change around 185 °C found by both SAXS and rheology is believed to be just the relaxation process from nonequilibrium LLP to BCC. We believe that the dominant LLP phase observed below 180 °C would completely transform to BCC phase after extensive annealing below this temperature (but still higher than 130 °C, the temperature we adopted in present work). However, the complete description of the annealing effect on the phase behavior of our V4113 is beyond the scope of this paper and thus will not be discussed further.

Figure 7 gives the change in synchrotron SAXS profiles of a 70/30 (w/w) V4113/PS2 mixture with temperature in semilogarithmic scale, and parts a and b of Figure 8 show  $1/I_{\max}$  and  $\sigma_q^2$  vs  $1/T$  and  $D$  vs  $1/T$  plots for this mixture, respectively. Similar to the SAXS results of pure V4113, all the scattering parameters for the 70/30 (w/w) mixture obviously show sharp discontinuities between 230 and 235 °C, indicating ODT. The value of the  $T_{ODT}$  is again in good agreement with the one determined from rheology. This mixture was also found to show OOT's from LAM to perforated lamellar (PL) or modulated lamellar (ML) phase between 166 and 172 °C and from PL or ML to HEX phase between 189 and 193 °C, which will be confirmed below by both SAXS and TEM.

In Figure 7, as temperature is increased, the second-order peak at a relative position 2 is observed to split into two peaks between 160 and 170 °C, and then its relative position changes from 2 to  $\sqrt{3}$  between 190 and 195 °C. The local maxima in both  $1/I_{\max}$  and  $\sigma_q^2$  vs  $1/T$  plots and the discontinuities in  $D$  vs  $1/T$  plot also exist between the same temperature ranges as indicated by



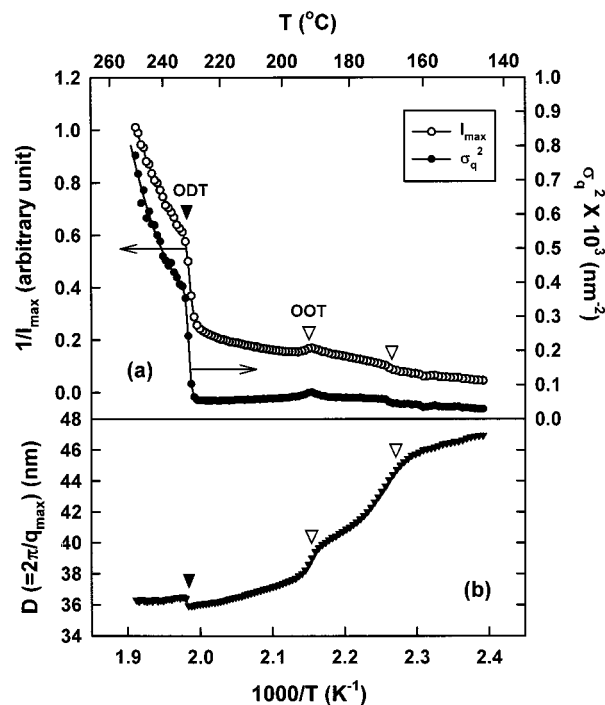


**Figure 8.** Scattering parameters as a function of inverse temperature for 70/30 (w/w) V4113/PS2 mixture: (a) inverse of the scattering maximum ( $1/I_{\max}$ ) and square of half-width at half-maximum ( $\sigma_q^2$ ) plotted against  $1/T$ ; (b) domain spacing ( $D = 2\pi/q_{\max}$ ) against  $1/T$ . A heating rate of  $1^{\circ}C/min$  was used.

the open arrows in parts a and b of Figure 8, respectively. These transition temperatures are consistent with the OOT temperatures determined from the change of  $\log G'$  as a function of  $T$ , as shown in Figure 3. Consequently, it can be concluded from the reports by other research groups<sup>28,33</sup> and our results except that of pure V4113 that the discontinuous change in  $D$  as well as the local maxima in both  $1/I_{\max}$  and  $\sigma_q^2$  against  $1/T$  can be attributed to OOT.

TEM micrographs of the two 70/30 (w/w) mixture samples, one quenched into liquid nitrogen after 2 h annealing at  $170^{\circ}C$  and the other after 30 min annealing at  $210^{\circ}C$  are shown respectively in parts a and b of Figure 9. The mixture clearly demonstrates the HEX phase at a high annealing temperature as shown in Figure 9b. Interestingly, however, the lamella-like structure at the annealing temperature of  $170^{\circ}C$  shown in Figure 9a is quite different from the true lamellar phase at the annealing temperature of  $130^{\circ}C$  shown in Figure 2d. Perforations in PS phase (which is the minor phase here) are identified by the difference in gray scale inside the bright PS phase although we cannot rule out the possible existence of modulations. As we mentioned above, the scattering profile at  $170^{\circ}C$  shown in Figure 7 shows the splitting of the second-order peak around the relative position 2 as indicated by thick and thin arrows. Note that the relative positions of the split peaks are 1.84 and 2.0, and the first-order peak shows a broad shoulder on the left side, which implies that the mixture has a new morphology rather than LAM or HEX. This second-order peak splitting as well as the first-order peak splitting has been attributed to the LAM/PL coexistence by Hajduk and co-workers.<sup>34,35</sup> They found using SAXS and TEM that polystyrene-poly(ethylene-*co*-butene) (SEB) diblock copolymer having  $f_{PS} = 0.28$  undergoes LAM  $\rightarrow$  LAM/PL  $\rightarrow$  PL/HEX  $\rightarrow$  HEX transitions with increasing

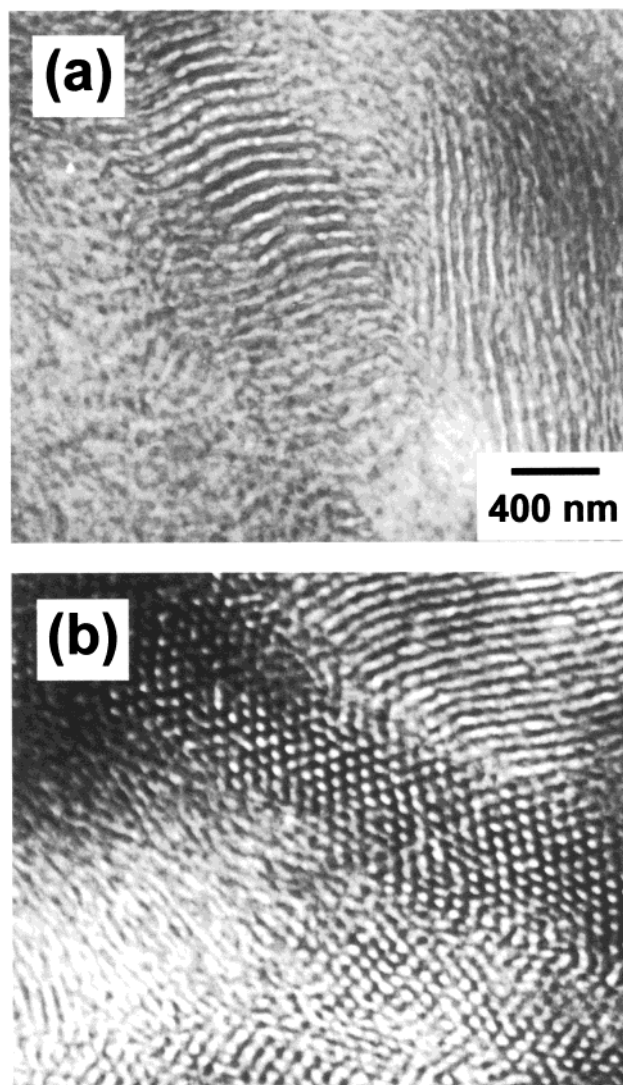


**Figure 9.** TEM micrographs of 70/30 (w/w) V4113/PS2 mixtures quenched into liquid nitrogen after annealing (a) at  $170^{\circ}C$  for 2 h and (b) at  $210^{\circ}C$  for 30 min.

temperature.<sup>34</sup> They also reported TEM micrographs similar to ours for various block copolymer systems having PL structure and found that PL is not thermodynamically stable but the long-lived metastable structure observed during the LAM  $\rightarrow$  HEX or LAM  $\rightarrow$  gyroid transitions.<sup>34,35</sup> The metastability of PL and/or ML phases was also investigated theoretically by Laradji et al.<sup>36</sup> using the anisotropic fluctuation theory. They found that LAM transforms into HEX via undulated lamellar phase and that experimentally observed PL and/or ML phases along the LAM/HEX phase boundary result from the infinitely degenerate fluctuation modes of LAM phase. Consequently, it can be inferred that our 70/30 (w/w) V4113/PS2 mixture transforms from LAM to HEX phase through an intermediate metastable PL or ML structure as temperature is increased. The existence of PL or ML structure for the 70/30 (w/w) mixture is believed to be due to the finite heating rate ( $1^{\circ}C/min$ ) in the SAXS measurements and the short annealing time of the sample for TEM. Unfortunately, our SAXS and TEM data are not sufficient to clearly identify between PL and ML phases. A complete description of PL or ML phases in our mixture samples, however, is beyond the scope of this paper and will not be discussed further.



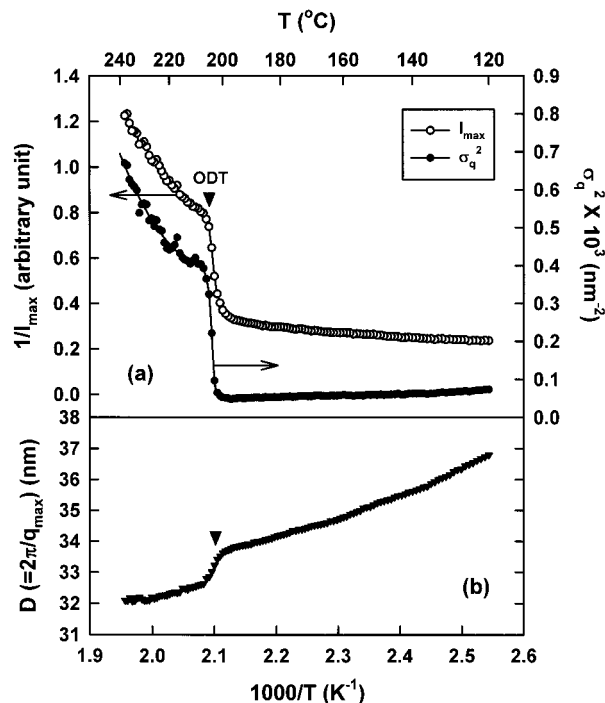


**Figure 10.** Scattering parameters as a function of inverse temperature for 90/10 (w/w) V4113/PS2 mixture: (a) inverse of the scattering maximum ( $1/I_{\max}$ ) and square of half-width at half-maximum ( $\sigma_q^2$ ) plotted against  $1/T$ ; (b) domain spacing ( $D = 2\pi/q_{\max}$ ) against  $1/T$ . A heating rate of  $1^{\circ}C/min$  was used.

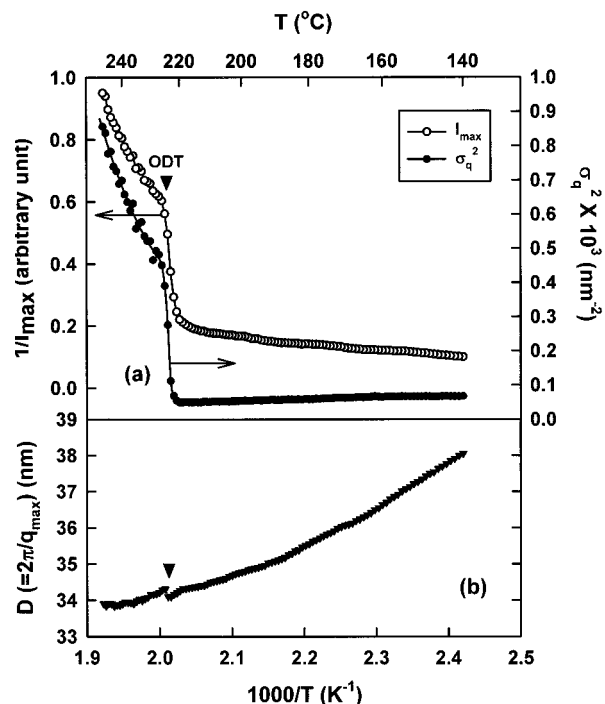


**Figure 11.** Scattering parameters as a function of inverse temperature for 80/20 (w/w) V4113/PS2 mixture: (a) inverse of the scattering maximum ( $1/I_{\max}$ ) and square of half-width at half-maximum ( $\sigma_q^2$ ) plotted against  $1/T$ ; (b) domain spacing ( $D = 2\pi/q_{\max}$ ) against  $1/T$ . A heating rate of  $1^{\circ}C/min$  was used.

$1/I_{\max}$ ,  $\sigma_q^2$ , and  $D$  vs  $1/T$  plots for 90/10 and 80/20 (w/w) V4113/PS2 mixtures were also obtained from the scattering profiles of the mixtures (not shown here) and presented in Figures 10 and 11, respectively. Similarly, a discontinuity in the  $D$  vs  $1/T$  plot as well as in the  $1/I_{\max}$  and  $\sigma_q^2$  vs  $1/T$  plots was found at ODT for both

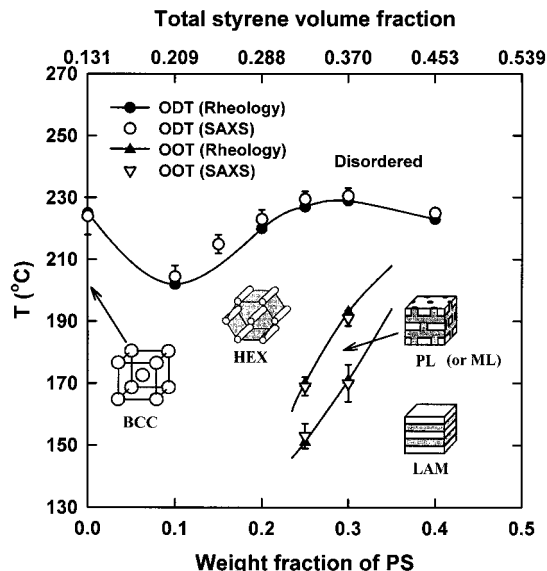


**Figure 12.** Phase diagram of V4113/PS2 mixtures. Filled and open symbols are  $T_{ODT}$ 's (or  $T_{OOT}$ 's) obtained from rheological and SAXS measurements, respectively.

mixtures. The  $T_{ODT}$  values were again in good agreement with the ones determined from the precipitous drop in  $\log G$  vs  $T$  plots shown in Figure 3. OOT was not observed in these mixtures, as evidenced by the absence of appreciable change in SAXS parameters ( $1/I_{\max}$ ,  $\sigma_q^2$ , and  $D$ ) and rheological property ( $G'$ ) other than at ODT.

**Phase Diagrams of Mixtures of SIS Triblock Copolymer and PS Homopolymers.** A complex phase diagram of the V4113/PS2 mixtures showing both ODT and OOT obtained from both SAXS and rheology is constructed in Figure 12. The type of microphase structure in each ordered region confirmed by TEM and SAXS is also indicated in the figure. The relaxation of pure V4113 from LLP to BCC phase is not included in the figure since it is not believed to be the equilibrium transition. PS2 homopolymer weight fraction of the mixture is converted to the overall styrene volume fraction  $\Phi_{PS}$  by assuming complete solubilization of PS2 in the polystyrene microdomain of the SIS triblock copolymer, and  $\Phi_{PS}$  is indicated in the upper  $x$ -axis. As we have previously mentioned,  $T_{ODT}$ 's of the V4113/PS2 mixtures determined from SAXS measurements are in good agreement with the ones determined from the  $\log G'$  vs  $T$  plots.

It is interesting to note that the value of  $T_{ODT}$  shows a minimum at 10 wt % of PS2. To the best of our knowledge, this abnormal behavior in ODT of block copolymer/homopolymer mixture system has not been reported previously. It has been reported that  $T_{ODT}$  just increases as homopolymer is added if the molecular weight ratio of homopolymer to block copolymer,  $\alpha$ , is larger than a certain critical value or simply decreases in the opposite case.<sup>1,13-18</sup> Even compositionally asymmetric block copolymers have shown the same trend with the homopolymer addition although the critical value of  $\alpha$  depends on the asymmetry.<sup>17,18</sup> Our previous study<sup>37</sup> on the ODT of the mixtures of nearly symmetric SIS triblock copolymer with  $f_{PS} = 0.371$  and PS homopolymer also showed that the ODT just increased or decreased depending on  $\alpha$ .

In addition to the ODT, it can be clearly seen in Figure 12 that the 75/25 (w/w) V4113/PS2 mixture

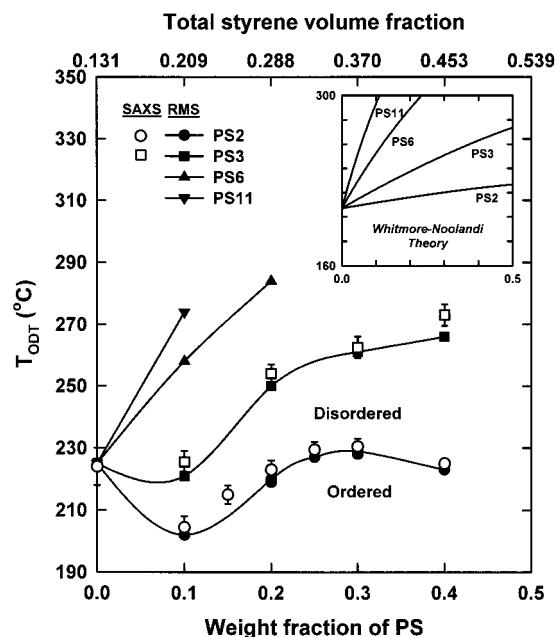


**Figure 13.** Phase diagrams of V4113/PS mixtures with different PS molecular weight. Filled and open symbols are  $T_{ODT}$ 's obtained from rheological and SAXS measurements, respectively. Calculations based on the Whitmore–Noolandi theory are also shown in the inset.

having  $\Phi_{PS} = 0.328$  shows OOT's from LAM to PL or ML phase around 150 °C and from PL or ML to HEX phase around 170 °C. The 70/30 (w/w) mixture having  $\Phi_{PS} = 0.370$  shows a similar phase sequence around 168 and 190 °C. As we mentioned before, the PL or ML phase found during the LAM  $\rightarrow$  HEX transition seems to be the intermediate metastable phase. A narrow range of the overall styrene volume fraction of the mixtures showing the complex ordered phases,  $0.328 \leq \Phi_{PS} \leq 0.370$ , agrees well with that of  $f_{PS}$  reported for pure SI diblock copolymers,<sup>9</sup>  $0.32 \leq f_{PS} \leq 0.35$ , although the range is slightly broader than that of SI diblock copolymers. This implies that the presence of homopolymer in the microdomain of block copolymers stabilizes the complex ordered phases.<sup>14</sup>

Before explaining in detail the origin of the complex phase behavior of V4113/PS2 mixtures, we will first describe the effect of molecular weight of added PS homopolymer on the ODT. We carried out the same experimental procedure described above for mixtures of V4113 with PS3, PS6, and PS11 having higher molecular weights than PS2. Phase diagrams of V4113/PS mixtures with different PS molecular weights obtained from both rheological and SAXS measurements are given in Figure 13. The overall styrene volume fractions calculated as previously described are again shown in the upper x-axis. SAXS measurements of the ODT were conducted only for mixtures with PS2 and PS3.  $T_{ODT}$ 's of V4113/PS3 mixtures determined from SAXS measurements are also in good agreement with the ones determined from the  $\log G$  vs  $T$  plots. The phase diagram of V4113/PS3 mixtures shows a similar trend to that of the V4113/PS2 mixtures;  $T_{ODT}$  shows the minimum at 10 wt % of PS3. On the other hand,  $T_{ODT}$ 's of the mixtures with PS6 and PS11 simply increase as PS is added. The increase in PS molecular weight was found to cause the increase in  $T_{ODT}$  of the mixture at a fixed composition.

Theoretical phase diagrams were also constructed in the inset of Figure 13 based on the Whitmore–Noolandi theory<sup>1</sup> for comparison with the experimental results. The following expression was used to take into account the temperature-dependent Flory–Huggins interaction parameter  $\chi$  between styrene and isoprene segments.<sup>38</sup>

$$\chi = -0.0419 + 38.54/T \quad (2)$$

It should be noted here that no adjustable parameter was used in the above calculations.

It was found from our previous study<sup>37</sup> that the Whitmore–Noolandi theory excellently predicted the phase diagrams of a series of binary mixtures of symmetric SIS triblock copolymer ( $f_{PS} = 0.371$ ) having lamellar microdomain and PS homopolymers with different molecular weights. Although the theory assumed that microdomain morphology is always lamellar regardless of block composition and homopolymer fraction, it also reasonably predicts the phase behavior of some of our asymmetric block copolymer/homopolymer mixtures as displayed in Figure 13. The predicted  $T_{ODT}$ 's of V4113/PS6 and V4113/PS11 mixtures increase as PS homopolymer is added, which is consistent with the experimental phase diagrams. On the other hand, the abnormal phase behavior of V4113/PS2 and V4113/PS3 mixtures showing the minimum in ODT at 10 wt % PS is not consistent with the theoretical predictions. Even recent theories<sup>14,15</sup> incorporating the change in microdomain morphology other than lamellae cannot predict this behavior.

We assumed in the above calculations that  $\chi$  is a function of temperature only. Tanaka and Hashimoto,<sup>39</sup> however, reported that  $\chi$  for the mixtures of PS–PI diblock copolymer and PS homopolymer depends not only on temperature but also on volume fraction and relative molecular weight of homopolymer, although their analysis of  $\chi$  was complicated due to the dilution approximation since they used dioctyl phthalate as a solvent in order to reduce  $T_{ODT}$ . Recently, Maurer et al.<sup>40</sup> found that the composition-independent expression of  $\chi$  for PE/PEP blends is quite different from the expressions of  $\chi$  for a series of symmetric PE–PEP diblock copolymers. They attributed this disparity to the *chain stretching effect* of block copolymers in the vicinity of ODT. Their result also implies that  $\chi$  for the mixtures of block copolymer and homopolymer depends on the volume fraction and molecular weight of homopolymer since the added homopolymer would affect the chain stretching of the block copolymer.

To check the above argument for our mixtures, we calculated structure parameters for each microdomain of V4113/PS2 mixtures at the same temperature of 200 °C, which is near but below  $T_{ODT}$ , based on the SAXS results. Table 2 summarizes the calculated structure parameters. The radius of BCC spherical or HEX cylindrical microdomains of PS,  $R_{PS}$ , is calculated by the following relations:<sup>41</sup>

$$R_{PS} = D \left( \frac{2}{\sqrt{3}\pi} \Phi_{PS} \right)^{1/2} \quad \text{for HEX} \quad (3)$$

$$R_{PS} = \frac{D}{\sqrt{2}} \left( \frac{3}{\pi} \Phi_{PS} \right)^{1/3} \quad \text{for BCC} \quad (4)$$

where we assume perfect BCC or HEX packing and complete solubilization of PS homopolymer into the PS microdomain of block copolymer. On the basis of geo-



**Table 2. Structure Parameters for Microdomains of V4113/PS2 Mixtures at 200 °C Obtained from SAXS**

V4113/PS2 (w/w)	microdomain morphology	$\Phi_{PS}^a$	$D^b$ (nm)	$R_{PS}^c$ (nm)	$L_{PI}^d$ (nm)
100/0	BCC	0.131	30.92	10.93	16.00
90/10	HEX	0.209	33.64	9.32	20.20
80/20	HEX	0.288	34.78	11.32	17.52
70/30	HEX	0.370	37.39	13.79	15.59

<sup>a</sup> Overall styrene volume fraction, calculated by assuming complete solubilization of PS2 in the polystyrene microdomains of block copolymer. <sup>b</sup> Domain periodicity,  $D = 2\pi/q_{max}$ . <sup>c</sup> Radius of BCC spherical or HEX cylindrical microdomains of PS, calculated by eqs 3 or 4. <sup>d</sup> Distance between outer surfaces of nearest PS microdomains, calculated by eqs 5 or 6.

metrical consideration, the distance between outer surfaces of nearest PS microdomains,  $L_{PI}$ , is then given as

$$L_{PI} = \frac{2}{\sqrt{3}} D - 2R_{PS} \quad \text{for HEX} \quad (5)$$

$$L_{PI} = \frac{\sqrt{6}}{2} D - 2R_{PS} \quad \text{for BCC} \quad (6)$$

$L_{PI}$  is closely related to PI chain stretching since a large portion of our triblock copolymers can form *bridge* structures through this distance, connecting the PS microdomains together. As shown in Table 2,  $D$  slightly increases as PS2 is added, but  $R_{PS}$  and  $L_{PI}$  show the minimum and maximum, respectively, at 10 wt % of PS2. Although the microdomain morphology changes from BCC to HEX when PS2 is added, the maximum of  $L_{PI}$  at 10 wt % of PS2 really implies that the chain stretching of PI block is maximized at this composition. This explains in part the minimum of ODT at this composition and the discrepancy between theoretical predictions and our experimental results. This argument is also supported by the fact that  $D$ 's of 100/0, 80/20, and 70/30 (w/w) V4113/PS2 mixtures show the discontinuous increase at ODT with increasing temperature as noted from Figures 5b, 11b, and 8b while the  $D$  of 90/10 (w/w) mixture shows the opposite trend as shown in Figure 10b. According to Matsen and Bates,<sup>33</sup> the abrupt increase in  $D$  at ODT is expected due to the fact that the short minority blocks, which are poorly anchored to their spherical or cylindrical domains, are pulled free to the matrix, thus swelling the majority domain at ODT. In the case of the 90/10 (w/w) mixture, we believe, however, that there is a prevailing tendency of the strongly stretched PI chains of the SIS triblock copolymer to relax back to the Gaussian conformations after the microphase disorders and thus contracting the majority PI domains at ODT. This would cause a decrease in  $D$  at ODT.

Adding homopolymer to the lamellar microdomains of symmetric block copolymer has usually been known to have two competing effects on the ODT.<sup>15</sup> One is the *disordering effect* by increasing the mixing entropy due to the random distribution of added homopolymer inside the microdomain of a block copolymer, and the other is the *ordering effect* by relieving stress within the microstructure. The former is dominant for systems with low molecular weight homopolymers since they have a tendency to be solubilized *uniformly* into the microdomains,<sup>2</sup> thus decreasing  $T_{ODT}$ . On the other hand, the latter case is dominant for systems with high molecular weight homopolymers since they tend to be *localized* to

the center of the microdomains,<sup>2</sup> thus increasing  $T_{ODT}$ . This argument is also applicable to the asymmetric block copolymers forming HEX or BCC microdomains, although much smaller molecular weight homopolymer is needed for the former effect to be dominant when a homopolymer is added to a minority component of a block copolymer.

For highly *asymmetric* block copolymer systems such as the present case, however, the *packing frustration* can also play an important role in the ordering. Packing frustration<sup>42,43</sup> has been reported for asymmetric systems with curved interface and described as a tendency to form domains of uniform thickness so that none of the constituent molecules are excessively stretched. Addition of a homopolymer to a majority domain of an asymmetric block copolymer has been reported to reduce this packing frustration since the added homopolymer fills the corners of Wigner-Seitz cell.<sup>42,43</sup> On the other hand, the effect of adding homopolymer to the minority domain has not been clearly understood yet. The packing frustration in our system is also believed to be closely related to the *PI chain stretching* ( $L_{PI}$  in Table 2). It seems that the packing frustration in the majority domain (PI phase) of V4113/PS2 mixtures reaches the maximum around 10 wt % of PS2 since the PI chains already stretched excessively should stretch even more in order to fill the space uniformly. The other two effects mentioned above seem to cancel out for these mixtures, thus causing a minimum in ODT around 10 wt % of PS2. For V4113/PS6 and V4113/PS11 mixtures, however, the ordering effect by relieving stress within the microstructures is dominant, and the packing frustration becomes negligible. This results in the monotonic increase of ODT as shown in Figure 13. Consequently, we tentatively conclude that the packing frustration also accounts in part for the abnormal phase behavior of our system.

Finally, we should briefly mention here that the minimum in ODT is different from the isotropic Lifshitz point<sup>44</sup> recently observed in ternary blends of two homopolymers and a block copolymer although the isotropic Lifshitz point shows a similar minimum in the phase diagram. The isotropic Lifshitz point is a point at which the macrophase separation line intersects the microphase separation line. However, macrophase separation was not observed in our system. Consequently, the minimum in ODT of our system is not related to the isotropic Lifshitz point.

#### 4. Conclusion

Triblock copolymer/homopolymer mixtures showing no macrophase separation have been prepared by adding a small amount of a series of low molecular weight polystyrenes (PS) to a *compositionally asymmetric* polystyrene-*block*-polyisoprene-*block*-polystyrene copolymer, V4113 ( $\Phi_{PS} = 0.131$ ). The ODT and OOT of these mixtures were investigated by combining TEM, SAXS, and rheology.

ODT temperatures of the mixtures were first determined from the discontinuous change in  $\log G'$  vs  $T$  plots using rheology. They were found to be in good agreement with the ones determined from the discontinuous change in  $1/I_{max}$ ,  $\sigma_q^2$ , and  $D$  vs  $1/T$  plots using SAXS. OOT was also identified for 70/30 and 75/25 (w/w) V4113/PS2 mixtures having  $\Phi_{PS} = 0.328$  and 0.370, respectively, as evidenced from the change in  $\log G'$  vs  $T$  plots. The existence of the OOT was further supported

by the change in the relative position of higher order scattering peaks as well as the discontinuity in  $D$  and local maxima in  $1/I_{\max}$  and  $\sigma_q^2$  at the same temperatures. This was further confirmed by TEM for samples quenched from temperatures below and above OOT. A complex phase diagram of the V4113/PS2 mixtures was constructed on the basis of these results. First, pure V4113 was observed to undergo a relaxation process from LLP to BCC phase as temperature was increased. This abnormal behavior of V4113 was attributed to the nonequilibrium LLP phase caused by the lack of annealing. V4113 seems to require an extended annealing at a temperature much higher than  $T_{g,PS}$  unlike other mixture samples having HEX or LAM morphology presumably due to the slow ordering rate of its spherical microdomains. Second, 70/30 and 75/25 (w/w) V4113/PS2 mixtures showed the complex phase sequence LAM  $\rightarrow$  PL (or ML)  $\rightarrow$  HEX. The PL (or ML) phase seems to be the intermediate metastable state during the LAM to HEX transition.

Phase diagrams of V4113/PS mixtures with different PS molecular weights were also constructed from the ODT measurements using both SAXS and rheology and compared with theoretical predictions based on the Whitmore–Noolandi theory. Unlike the mixtures of a compositionally symmetric block copolymer and a homopolymer, ODT of V4113/PS2 mixtures first decreased and increased again with the addition of PS2. To the best of our knowledge, this kind of phase behavior has not been reported and is inconsistent with predictions from any existing theories. We attribute this abnormal phase behavior to the *chain stretching* and/or *packing frustration* effects, which are usually negligible in normal block copolymer/homopolymer mixtures, with the addition of a low molecular weight homopolymer to the minority domain of a *highly asymmetric* triblock copolymer.

**Acknowledgment.** This work was partially funded by the Korean Ministry of Science and Technology (MOST) under Grant 99-07 and the Korean Ministry of Education through the Brain Korea 21 Program. SAXS experiments performed at Pohang Light Source (PLS) were supported in part by MOST and POSCO. We are very grateful to Y. J. Park and I. Lee for their assistance during SAXS experiments at PLS. We also thank C. Y. Ryu at University of California, Santa Barbara, U.S.A., for his valuable comments on this work. G. Kim thanks Prof. M. Libera in the Department of Chemical, Biochemical and Materials Engineering at Stevens Institute of Technology, Hoboken, NJ, for kindly providing TEM facilities.

## References and Notes

- Whitmore, M. D.; Noolandi, J. *Macromolecules* **1985**, *18*, 2486.
- Tanaka, H.; Hasegawa, H.; Hashimoto, T. *Macromolecules* **1991**, *24*, 240.
- Mayes, A. M.; Russell, T. P.; Satija, S. K.; Majkrzak, C. F. *Macromolecules* **1992**, *25*, 6523.
- Jeon, K.-J.; Roe, R.-J. *Macromolecules* **1994**, *27*, 2439.
- Leibler, L. *Macromolecules* **1980**, *13*, 1602.
- Fredrickson, G. H.; Helfand, E. *J. Chem. Phys.* **1987**, *87*, 697.
- Rosedale, J. H.; Bates, F. S. *Macromolecules* **1990**, *23*, 2329.
- Bates, F. S.; Rosedale, J. H.; Fredrickson, G. H. *J. Chem. Phys.* **1990**, *92*, 6255.
- Khandpur, A. K.; Förster, S.; Bates, F. S.; Hamley, I. W.; Ryan, A. J.; Bras, W.; Almdal, K.; Mortensen, K. *Macromolecules* **1995**, *28*, 8796.
- Sakamoto, N.; Hashimoto, T. *Macromolecules* **1995**, *28*, 6825.
- Han, C. D.; Baek, D. M.; Kim, J. K.; Ogawa, T.; Sakamoto, N.; Hashimoto, T. *Macromolecules* **1995**, *28*, 5043.
- Ogawa, T.; Sakamoto, N.; Hashimoto, T.; Han, C. D.; Baek, D. M. *Macromolecules* **1996**, *29*, 2113.
- de la Cruz, M. O.; Sanchez, I. C. *Macromolecules* **1987**, *20*, 440.
- Matsen, M. W. *Macromolecules* **1995**, *28*, 5765.
- Janert, P. K.; Schick, M. *Macromolecules* **1998**, *31*, 1109.
- Bodycomb, J.; Yamaguchi, D.; Hashimoto, T. *Polym. J.* **1996**, *28*, 821.
- Roe, R.-J.; Zin, W.-C. *Macromolecules* **1984**, *17*, 189.
- Baek, D. M.; Han, C. D.; Kim, J. K. *Polymer* **1992**, *33*, 4821.
- Tanaka, H.; Hashimoto, T. *Macromolecules* **1991**, *24*, 5713.
- Mani, S.; Weiss, R. A.; Hahn, S. F.; Williams, C. E.; Cantino, M. E.; Khairallah, L. H. *Polymer* **1998**, *39*, 2023.
- Matsuoka, H.; Tanaka, H.; Iizuka, N.; Hashimoto, T.; Ise, N. *Phys. Rev. B* **1990**, *41*, 3854.
- Kim, J. K.; Lee, H. H.; Sakurai, S.; Aida, S.; Masamoto, J.; Nomura, S.; Kitagawa, Y.; Suda, Y. *Macromolecules* **1999**, *32*, 6707.
- Funaki, Y.; Kumano, K.; Nakao, T.; Jinnai, H.; Yoshida, H.; Kimishima, K.; Tsutsumi, K.; Hirokawa, Y.; Hashimoto, T. *Polymer* **1999**, *40*, 7147.
- Lipic, P. M.; Bates, F. S.; Matsen, M. W. *J. Polym. Sci., Part B: Polym. Phys. Ed.* **1999**, *37*, 2229.
- Huang, C.; Chapman, B. R.; Lodge, T. P. *Macromolecules* **1998**, *31*, 9384.
- Yamaguchi, D.; Hashimoto, T.; Vaidya, N. Y.; Han, C. D. *Macromolecules* **1999**, *32*, 7696.
- Ryu, C. Y.; Vigild, M. E.; Lodge, T. P. *Phys. Rev. Lett.* **1998**, *81*, 5354.
- Sakamoto, N.; Hashimoto, T.; Han, C. D.; Kim, D.; Vaidya, N. Y. *Macromolecules* **1997**, *30*, 1621.
- Private communication with C. D. Han.
- Koga, T.; Koga, T.; Hashimoto, T. *J. Chem. Phys.* **1999**, *110*, 11076.
- Floudas, G.; Hadjichristidis, N.; Iatrou, H.; Pakula, T.; Fischer, E. W. *Macromolecules* **1994**, *27*, 7735.
- Floudas, G.; Pispas, S.; Hadjichristidis, N.; Pakula, T.; Erukhimovich, I. *Macromolecules* **1996**, *29*, 4142.
- Matsen, M. W.; Bates, F. S. *J. Polym. Sci., Part B: Polym. Phys. Ed.* **1997**, *35*, 945.
- Hajduk, D. A.; Gruner, S. M.; Rangarajan, P.; Register, R. A.; Fetters, L. J.; Honeker, C.; Albalak, R. J.; Thomas, E. L. *Macromolecules* **1994**, *27*, 490.
- Hajduk, D. A.; Ho, R.-M.; Hillmyer, M. A.; Bates, F. S.; Almdal, K. *J. Phys. Chem. B* **1998**, *102*, 1356.
- Laradji, M.; Shi, A.-C.; Noolandi, J.; Desai, R. C. *Macromolecules* **1997**, *30*, 3242.
- Lee, S.-H.; Char, K. In *ACS Symposium Series*; Cebe, P., Lohse, D. J., Hsiao, B. S., Eds.; American Chemical Society: Washington, DC, 1999; Vol. 739, Chapter 31.
- Hashimoto, T.; Ijichi, Y.; Fetters, L. J. *J. Chem. Phys.* **1988**, *89*, 2463.
- Tanaka, H.; Hashimoto, T. *Macromolecules* **1991**, *24*, 5398.
- Maurer, W. W.; Bates, F. S.; Lodge, T. P.; Almdal, K.; Mortensen, K.; Fredrickson, G. H. *J. Chem. Phys.* **1998**, *108*, 2989.
- Sakurai, S.; Kawada, H.; Hashimoto, T.; Fetters, L. J. *Macromolecules* **1993**, *26*, 5796.
- Turner, D. C.; Gruner, S. M. *Biochemistry* **1992**, *31*, 1340.
- Matsen, M. W.; Bates, F. S. *Macromolecules* **1996**, *29*, 7641.
- Bates, F. S.; Maurer, W.; Lodge, T. P.; Schulz, M. F.; Matsen, M. W.; Almdal, K.; Mortensen, K. *Phys. Rev. Lett.* **1995**, *75*, 4429.

MA000658X